PROCEEDINGS, 50th Workshop on Geothermal Reservoir Engineering
Stanford University, Stanford, California, February 10-12, 2025
SGP-TR-229

# Data-driven Lithium and Geothermal Resource Assessment in the Smackover Formation

Xiang Huang[1], Bulbul Ahmmed[1], Mohamed Mehana[1], Shuvajit Bhattacharya[2], Chelsea Neil[1]

[1]Earth and Environmental Sciences Division, Los Alamos National Laboratory, USA

[2]Bureau of Economic Geology, The University of Texas at Austin, USA

xhuang@lanl.gov

**Keywords:** Lithium, Smackover Formation Geothermal Field, Critical Minerals, Unsupervised Machine Learning Technique

## ABSTRACT

The Smackover Limestone Formation represents a vital resource for both geothermal energy and lithium (Li) recovery, especially as the demand for critical minerals and renewable energy continues to rise. This study leverages advanced artificial intelligence (AI) and machine learning (ML) techniques to optimize the identification, extraction, and co-production of Li from geothermal brines. The Smackover Formation has played a pivotal role in the U.S. energy sector for over a century, contributing significantly to the country's conventional energy economy. Since the 1950s, the region's brines have been commercially tapped for bromine, which is found in abundance within the deep sedimentary basins of the formation. These brines, however, also contain a complex array of valuable components, presenting new opportunities for the extraction of critical minerals such as lithium, potassium, boron, and iodine. Recent reports have identified lithium concentrations as high as 1,700 mg/L in these deep-basinal oilfield brines of the Gulf Coast.

Building upon extensive multi-dimensional datasets from the Smackover region, encompassing geological, geochemical, and geothermal data, this study employs Los Alamos National Laboratory's nonnegative matrix factorization with k-means clustering (NMFk) to uncover hidden signatures within the data. This enables the identification of lithium-rich zones and the development of optimized extraction strategies. Results indicate that TDS, SG, $Cl^-$, $K^+$, and $Na^+$ exhibit strong correlations with lithium, suggesting a robust geochemical relationship. Three hotspot regions for co-exploration of Li-Geothermal were identified using quantile-based categories superimposing Li concentration and temperature and with simplified interpolation methods. While the prospectivity distributions from NMFk and kriging methods show strong agreement, NMFk also highlights spatial variations among lithium signatures. For instance, Signature 5, which achieves the best fit, covers a smaller spatial extent compared to other signatures, reflecting the localized nature of lithium deposits. High lithium concentrations are primarily concentrated in southern Arkansas and northern Louisiana, whereas elevated temperatures dominate the Texas region, underscoring distinct geospatial patterns. We utilized both conservative and optimistic overlapping approaches to assess Li-geothermal co-resource prospectivity. The conservative approach constrains prospectivity, while the optimistic approach expands it. If the optimistic approach is adopted, a potential synergy between the two resources becomes evident, potentially leading to higher revenue generation.

## 1. INTRODUCTION

Our much of modern life and the global transition to a sustainable energy future depends on critical minerals. The Smackover Limestone Formation, a vast sedimentary basin along the Gulf Coast, presents a unique opportunity to address both challenges simultaneously. Historically recognized for its oil/gas and bromine production, the formation's deep oilfield brines are now garnering attention for their significant concentrations of lithium (Li) and other valuable elements, such as potassium, boron, and iodine (Worley, 2019; NORAM, 2021). Recent studies have reported lithium concentrations as high as 1,700 mg/L in these brines, highlighting their potential as a critical domestic lithium source (Darvari et al., 2024; Marza et al., 2024). With the ever-growing demand for lithium in battery technologies and renewable energy systems, developing optimized extraction methods from geothermal brines has become an urgent priority (Çetiner et al., 2015; Stringfellow & Dobson, 2021; Gibb, 2021; Yang et al., 2024).

Geothermal brine mining in the Smackover Formation has a rich legacy rooted in the U.S. energy sector. Since the 1950s, the region's brines have been commercially exploited for bromine (Collins, 1974; Worley, 2019). Between 1986 and 1990, the produced bromine supplied over 40% of the world's bromine supply and continues to account for a significant portion of global bromine production capacity (Schnebele, 2018; Worley, 2019). That same bromine-rich brine found in deep sedimentary basins contains complex components and offers the opportunity for harvesting critical minerals such as lithium, potassium, boron, and iodine (Collins, 1969; Nash, 2024). Today, these same brines offer new lithium recovery possibilities and could generate 750,000 metric tons of Li metal equivalents (Kumar et al., 2019). Lithium's distribution within the deep, thermally enriched reservoirs is influenced by variables such as brine chemistry, temperature, pressure, and reservoir geology. The Smackover Formation's favorable thermal gradient and substantial brine volumes position it as an ideal candidate for the co-production of geothermal energy and lithium. This dual opportunity enhances economic value and aligns with global initiatives to transition toward cleaner energy systems while mitigating the environmental impacts of conventional mining (Mends & Chu, 2023).

This study integrates an unsupervised machine learning technique to assess lithium's occurrence, distribution, and co-extraction potential within the Smackover Formation. By employing Los Alamos National Laboratory's (LANL) nonnegative matrix factorization with k-means clustering (NMFk), we analyze geological, geochemical, and geothermal datasets to identify lithium and geothermal co-resources prospectivity. These techniques reveal hidden patterns in the data, offering new insights into the factors driving lithium mobilization and its synergy with geothermal energy production.

The inverse distance weighting (IDW) and ordinary kriging (OK) interpolation can generate prospectivity maps. They prioritize closer values over distant ones. NMFk takes a more holistic approach to spatial analysis. Both IDW and OK assume that nearby points are more similar than those farther apart, leading to localized predictions that may not fully capture broader spatial patterns. In contrast, NMFk goes beyond mere distance-based interpolation by uncovering latent structures and relationships across the entire dataset. This allows it to identify patterns that extend beyond local proximities, making it more robust for complex spatial distributions. Additionally, NMFk models spatial variation and detects correlations with other attributes of interest, providing deeper insights into underlying geochemical or geological processes. This makes NMFk particularly useful for applications where both spatial and attribute-based relationships need to be considered, offering a more comprehensive and data-driven approach than traditional interpolation methods.

## 2. MATERIALS AND METHODS

### 2.1. Geological settings

The Smackover Formation, formed during the Late Jurassic, is a vast rock layer created under ancient seas. It spans Arkansas and extends along the Gulf Coast, covering Texas, Louisiana, Mississippi, Alabama, and Florida. The formation is divided into five assessment units (AUs), as shown in Figure 1a, each characterized by unique geological features, including carbonate shelves, fault zones, and areas shaped by ancient rivers. This formation holds significant untapped oil and gas reserves, estimated at 143 million barrels of oil and over 1 trillion cubic feet of natural gas, making it an essential target for energy exploration (Birdwell et al., 2024). A geological transect in Figure 1b shows the stratigraphic and facies distribution within the Smackover Formation and associated units (Buckner, Bossier, and Schuler Formations) from Southwestern Arkansas (updip area) to Northwestern Louisiana (downdip area) (Dickinson, 1968; Birdwell et al., 2024). Key features include red sandstone beds, conglomeratic beds, facies boundaries, and transitions between marine and nonmarine facies. The formation primarily consists of porous, permeable limestone, with partial or complete dolomitization in some areas. Thickness ranges from up to 1,000 feet in Texas, Arkansas, Louisiana, and Mississippi to 100–300 feet in Alabama. It suggests that southern Arkansas, where high Li concentrations exist, is shallower, but the true origin may be deeper if Li simply accumulates at this depth. Significant discoveries continue, with the origin of Li still under investigation, leading to various hypotheses (Ettehadi et al., 2024; Heydari & Baria, 2005).

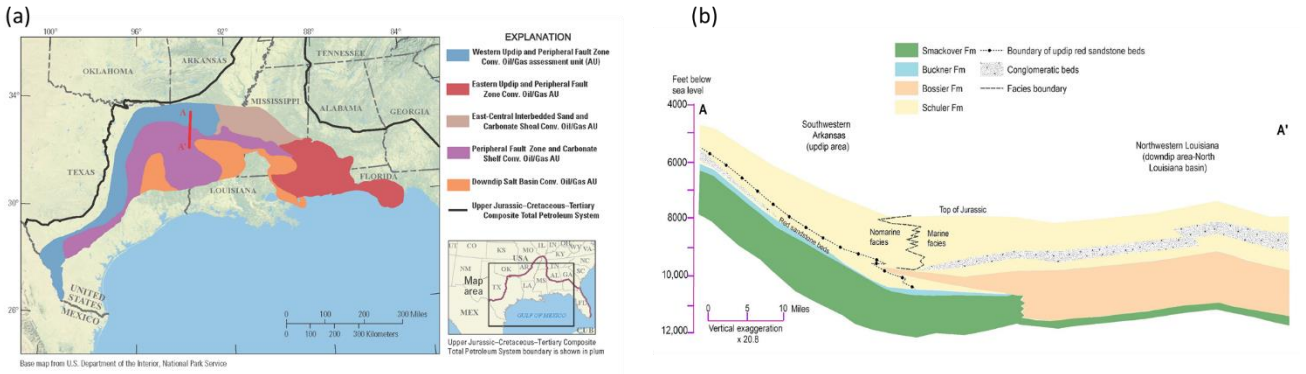


**Figure 1:** (a) Smackover Formation depositional extent with oil and gas assessment units (AUs) distribution (after Birdwell et al., 2024). (b) Cross section (A–A') shows the potential depth and extent of Smackover and other geological formations (after Sloan, 1958).

### 2.2. Data

The geochemical data used in this study are compiled from the published literature (Darvari et al., 2024; Marza et al., 2024; Attanasi et al., 2024; Knierim et al., 2024) and the USGS National Produced Waters Geochemical Database (Blondes et al., 2023). The dataset within the research domain covers 10,647 locations with 18 variables, including lithium and geothermal attributes. Among them, 3,380 are unique locations, and lithium has been identified at 540 sites, highlighting key resource areas.

The spatial distribution of lithium concentrations and geothermal temperatures in the Smackover Formation in Figure 2 reveals three distinct hotspots for the co-production of lithium and geothermal resources. These hotspots are in Arkansas (AR) and portions of northern Louisiana (LA), where high lithium concentrations (>83.97 mg/L) overlap with medium to high geothermal temperatures (≥100°C). In contrast, the southern areas, such as Texas (TX) and parts of Florida (FL), exhibit sparse or missing data, indicating a need for further exploration. This pattern underscores the potential for lithium and geothermal resource co-exploration in the identified hotspot regions, such as the border regions between Arkansas and northern Louisiana, while the southern areas may represent untapped opportunities for future investigation.

Figure 3 presents a statistical distribution of various geochemical parameters in the Smackover Formation, including Li, temperature, pH, total dissolved solids (TDS), major ions ($K^+$, $Ca^{2+}$, $Mg^{2+}$, $Na^+$, $HCO_3^-$, $SO_4^{2-}$), and trace elements ($Br^-$, $Cl^-$, Ba, Sr, $Fe_{total}$). The plots illustrate a wide range of values with significant variability, particularly in Li, Mg, and Na concentrations, which present long tails indicating the presence of extreme values. Median values (red lines) and interquartile ranges highlight central tendencies and variability for each parameter. The kernel density estimates show asymmetric distributions for several variables, suggesting non-normal data distributions, while the presence of outliers emphasizes the heterogeneous nature of the geochemical environment in the formation. Figure 4 shows the geospatial interpolation of lithium concentrations in the Smackover Formation. The Inverse Distance Weighting (IDW) method exhibits a sharper gradient between concentration zones, with abrupt changes in lithium values, whereas the Kriging method provides smoother transitions, reflecting the influence of spatial autocorrelation. While some specific locations are inaccurately represented, the general trends in lithium distribution are consistent across both methods. These results suggest that both interpolation approaches generally capture the overall spatial patterns, with Kriging offering a more geostatistically robust representation.

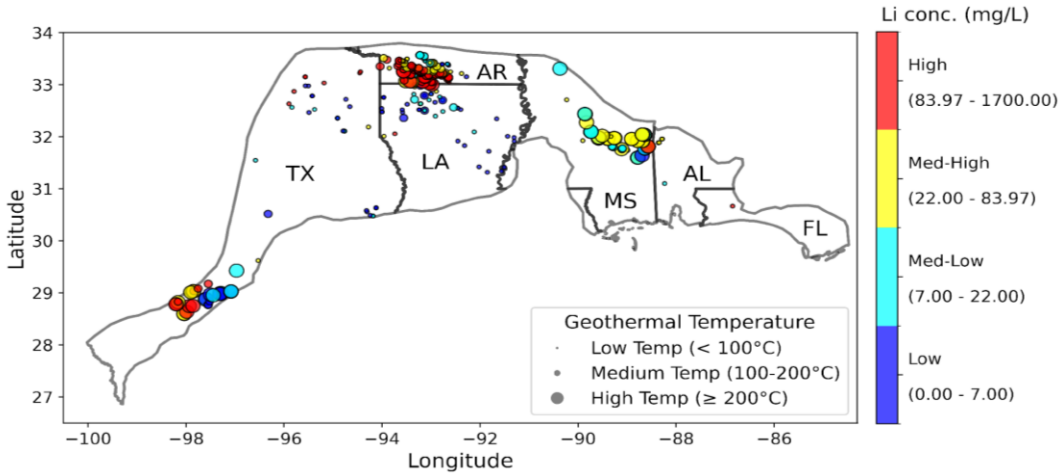


**Figure 2:** Spatial distribution of lithium concentrations and geothermal temperatures across the Smackover Formation. Lithium concentrations are represented by colored markers, ranging from low (blue, 0.00–7.00 mg/L) to high (red, 83.97–1700.00 mg/L). Geothermal temperatures are classified into low (<100°C), medium (100–200°C), and high (≥200°C), indicated by marker sizes.

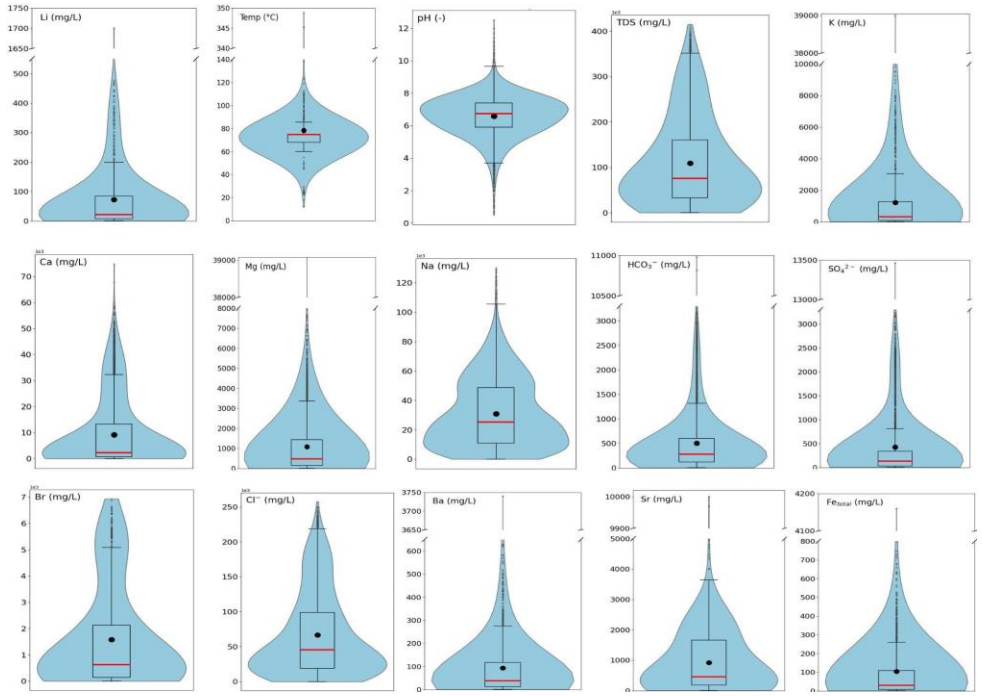


**Figure 3:** The statistical distribution of key geochemical variables in the Smackover Formation. Parameters include lithium concentration (Li, mg/L), temperature (Temp, °C), pH, total dissolved solids (TDS, mg/L), major ions ($K^+$, $Ca^{2+}$, $Mg^{2+}$, $Na^+$, $HCO_3^-$, $SO_4^{2-}$, mg/L), trace elements ($Br^-$, $Cl^-$, Ba, Sr, $Fe_{total}$, mg/L). Each plot displays each variable's concentration range, median (red line), mean (black dot), interquartile range, and kernel density, highlighting variability and central tendencies in the dataset.

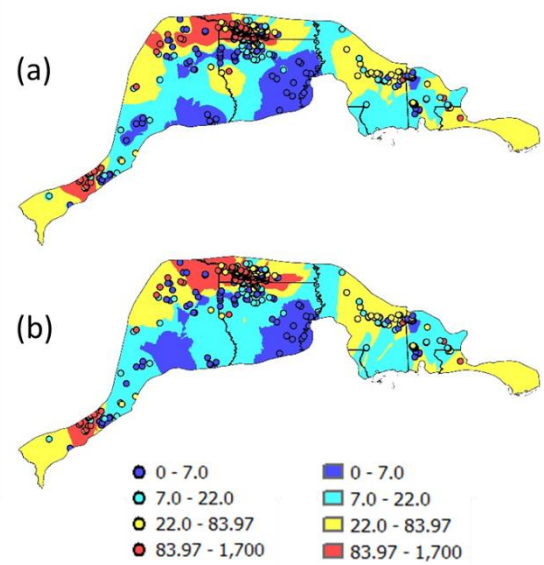


**Figure 4:** Comparison of lithium concentration geospatial interpolations in the Smackover Formation using (a) Inverse Distance Weighting (IDW) and (b) Ordinary Kriging methods. Both methods visualize lithium concentration with the quantile-based categories: 0–7.0 (blue), 7.0–22.0 (light green), 22.0–83.97 (yellow), and 83.97–1700 (red). Data points are represented by circles, highlighting observed lithium concentrations.

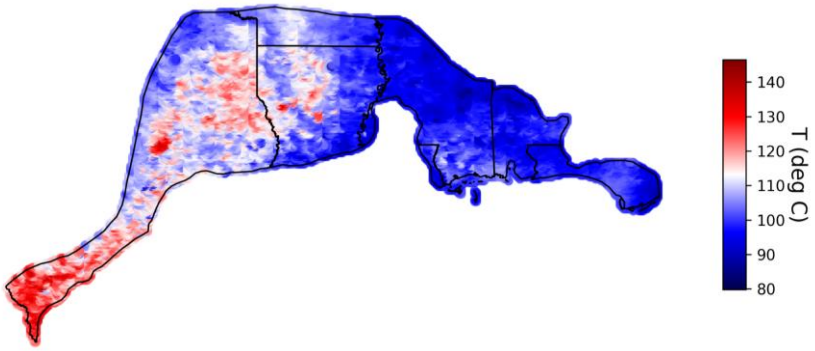


**Figure 5**: Temperature distribution in the Smackover region at 3000 m depth (source: Aljubran & Horne 2024).

Figure 5 illustrates the temperature distribution in the Smackover Formation at a depth of 3,000 m. The map reveals significant spatial variability in geothermal gradients, with higher temperatures (≥140°C) predominantly concentrated in the southern Texas region, shown in red. In contrast, cooler temperatures (90–100°C) are more widespread across northern Louisiana, southern Arkansas, and parts of Mississippi and Alabama, represented in shades of blue. These temperature patterns align with known geological and thermal characteristics of the region, highlighting the Smackover Formation's potential for geothermal energy exploitation, particularly in high-temperature zones. The spatial separation between high-temperature areas and lithium-rich zones, observed in previous analyses, suggests distinct resource optimization strategies may be required for co-production in this region.

2.3. Method

We used two machine learning methods called nonnegative matrix factorization (NMF) and k-means clustering to group and identify spatial patterns in the data. After receiving the outputs, we generated a Li prospectivity map and utilized a geothermal prospectivity map (cite) followed by overlapping of these two variables to find the Li and geothermal co-resources prospectivity map. NMF factorizes a data matrix, $X$, representing measurement locations and data attributes. The goal of NMF is to reduce the data dimension and find the optimal number of signatures $k$ capturing characteristics in the data set. There are several ways to factorize a data matrix. Here, we used multiplicative update for NMF that follows:

$$W \leftarrow W \cdot \frac{(VH^T)}{(WHH^T)} \tag{1}$$

$$H \leftarrow H \cdot \frac{(W^T V)}{(W^T W H)} \quad (2)$$

where *V*, *W*, and *H* represent data, attribute, and spatial matrices, respectively. Factorization starts with random positive values of *W* and *H*. The number of signatures *k* ranges between 2 and minimum data dimension. For a given number of signatures $k$, Equations 1 - 2 are iteratively solved by minimizing the reconstruction error $O(k)$:

$$O(k) = || X - W \times H||_F \quad (3)$$

by constraining the *W* and *H* elements to be greater or equal to zero and *F* defines the Frobenius matrix norm (Böttcher & Wenzel, 2008). NMF is executed at specified times generating a series of solutions for *W* and *H* matrices for a given *k* value. The resulting multiple solutions *H* are clustered into *k* clusters using a customized $k$-means clustering and the average silhouette width $S(k)$ based on the cosine norm is computed to know the robustness of clusters (Vesselinov et al. 2018).

NMF and k-means clustering provide a robust way to compare the accuracy of data reconstruction because NMF confirms the accuracy of data reconstruction while k-means clustering assures the quality of clusters. This method provides a solid understanding in both attribute and spatial domains. *W* and *H* help understand the relationship between signatures to locations and attributes, respectively. The location matrix, *W*, helps to plot the results that can be defined as prospectivity maps. However, here we only find the Li prospectivity map. To find the co-resources prospectivity map, we overlapped the Li prospectivity map with the recent geothermal prospectivity map (Aljubran & Horne 2024) in conservative and optimistic ways. As a conservative step, geothermal and Li prospectivities were multiplied to make the co-resources prospectivity map. For optimistic step, we added both prospectivities.

## 3. RESULTS

The reconstruction error, *O(k)*, decreases as the number of signatures increases, as a higher-dimensional representation allows for better reconstruction (Figure 6). However, the average silhouette width, S(k), fluctuates without following a distinct pattern. Generally, solutions with *S(k)>0.5* are considered reasonable (Ahmmed & Vesselinov, 2021). We ran the algorithm for 2 to 10 signatures, and all resulted in S(k)>0.5, indicating well-defined clusters across solutions. This suggests that the dataset can be effectively explained using any of these signature counts. However, an optimal solution should balance dimensionality avoiding excessive compression while preventing unnecessary complexity. For the given dataset, a signature count of 5 emerges as the optimal choice, as it achieves both a low reconstruction error *O(k)* and an almost perfect silhouette score, effectively capturing the dataset's characteristics.

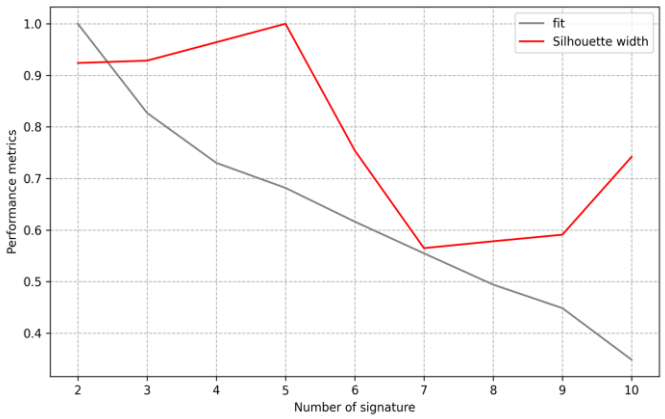


**Figure 6**: Normalized performance of different signatures where fit represents the reconstruction error and Silhouette width is clustering or grouping.

Li is dominant in the 2nd, 4th, and 4th signatures of solutions 4, 5, and 6, respectively (Figure 8), which we refer to as Li signatures. Among these, solution 4 offers a simplified representation, solution 5 provides an optimal balance, and solution 6 represents a more complex depiction of the data. While all three signatures effectively capture the dataset, simplified versions may introduce spurious correlations, whereas more complex versions incorporate additional details that may not be necessary. Given this trade-off, we focus on solution 5, as it strikes the best balance between interpretability and accuracy.

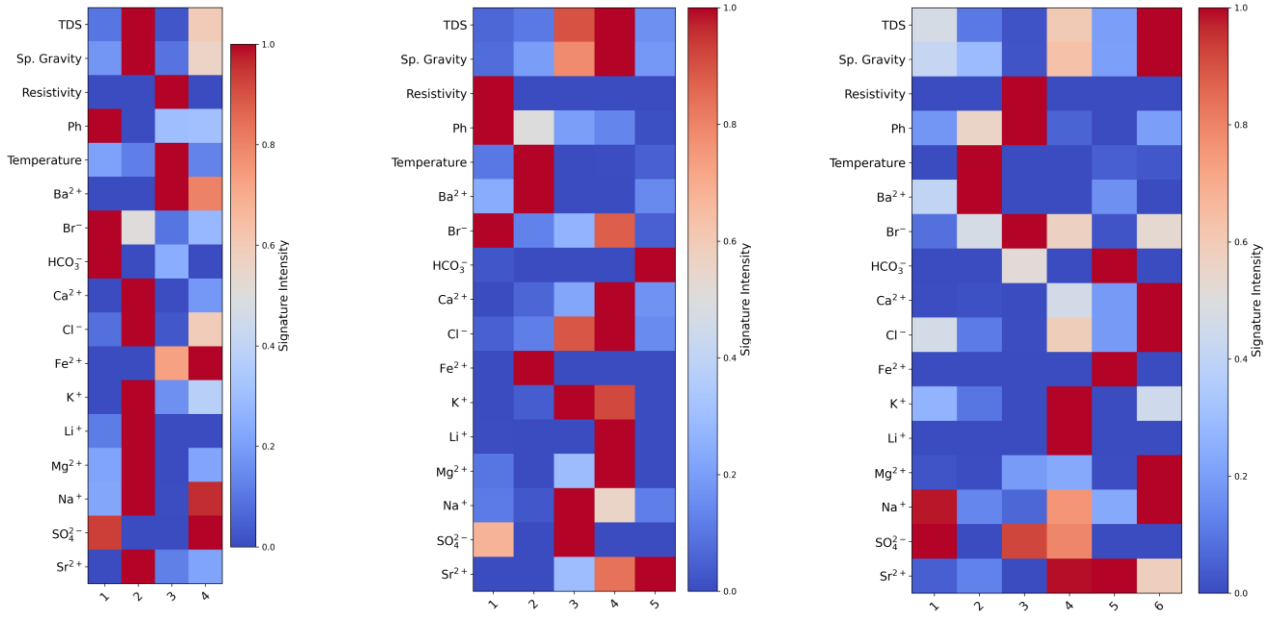


**Figure 7**: NMFk derived signatures of the Smackover lithium data. The left, center, and right figures represent the compressed version of the actual data with four, five, and six signatures, respectively.

Figure 7 (center) illustrates the correlation of various attributes with different signatures, where red-colored cells indicate high correlation, meaning these attributes strongly contribute to the corresponding signature. In signature, resistivity, pH, and $Br^{-}$exhibit strong correlations, suggesting they could be physicochemical properties of produced water. Signature 2 shows high correlation with temperature and $Ba^{2+}$, indicating their dominance. $Ba^{2+}$ is highly likely to indicate deep water flow and is hence highly correlated with temperature. $Li^{+}$ and $Fe^{2+}$ are highly correlated in signature 3, making them key factors in this signature's formation. This is indicative of trace metal characteristics of the dataset. Signature 4 has strong correlations with $Li^{+}$, TDS, Sp. Gravity, $Br^{-}$, $Cl^{-}$, $Ca^{2+}$, $Mg^{2+}$, and $K^{+}$ suggest that these attributes are crucial in shaping this representation. Lastly, signature 5 shows a high correlation with $HCO_3^{-}$ and $Sr^{2+}$.

Our primary focus is on Signature 4 due to its high intensity of Li, indicating that the locations associated with this signature have elevated Li concentrations. While TDS and Sp. Gravity represents physicochemical properties, their correlation with Li lacks a clear logical explanation. Other highly correlated variables, including $Br^{-}$, $Cl^{-}$, $Ca^{2+}$, $Mg^{2+}$, and $K^{+}$, primarily reflect cation-anion balance. The presence of Li in this correlation may be coincidental, or it may be an indicative relationship. However, the most critical finding is the correlation between $Li^{+}$ and $Sr^{+}$, as both are trace metals and remain consistently correlated across Signatures 4 to 6. Additionally, the absence of groundwater temperature in any solution where Li intensity is high suggests that Li and groundwater temperature are not correlated.

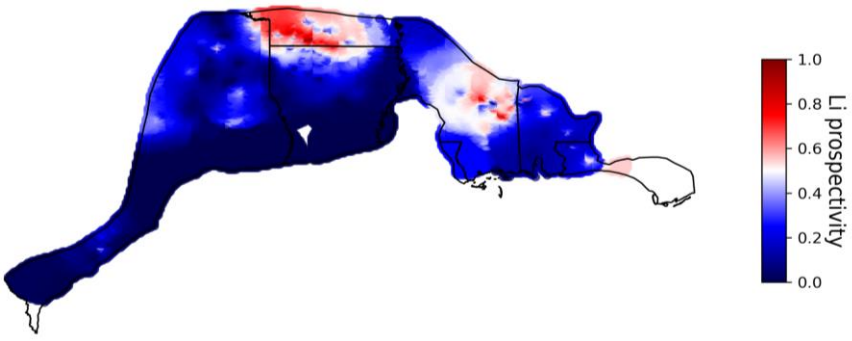


**Figure 8**: Li distribution in the Smackover region based on the USGS-produced water data.

Finally, we plotted signature 4 on a spatial map demonstrating their spatial distribution (Figure 8). There are two major hotspots; the first hotspot is around south Arkansas and north Louisiana, and the second is in central Mississippi. There are several spotty hotspots without significant presence. There is a little difference between Figure 8 and Figures 4a-b. Figures 4a and 4b are inverse distance weighting and ordinary kriging interpolation maps of Li. Figures 4a and 4b have three hotspots, with an extra one in east Texas. It would be unreasonable to claim which is better because these maps are produced with different techniques. Inverse distance weighting and ordinary kriging interpolate Li concentration, while the NMF-produced map does not have direct interpolation. Instead, it is more of a filtered version of

Li concentration. During the factorization process, NMF looks for correlation among all highly concentrated Li values and keeps only those that are spatially correlated.

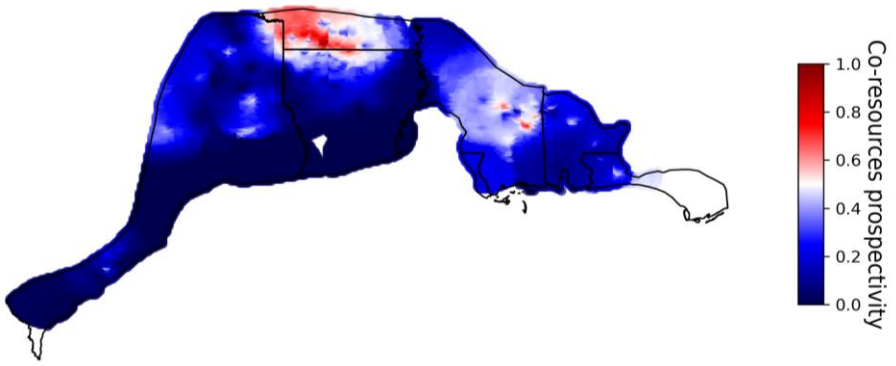


**Figure 9**: Conservative Li and geothermal dual-resource distribution in the Smackover region based on the USGS produced water data and Stanford produced geothermal prospectivity map.

Moreover, we overlaid Figures 5 and 8 by multiplying them and plotted the results to visualize the co-distribution of Li and geothermal resources. The resulting distribution closely mirrors the Li distribution but with a lower magnitude (Figure 9), indicating that the overlap between temperature and Li did not enhance the signature. Instead, their interaction has a negative impact, as their dominant regions do not align well. For example, geothermal prospectivity is relatively low in southern Arkansas, whereas Li prospectivity is high in the same area, highlighting their spatial mismatch.

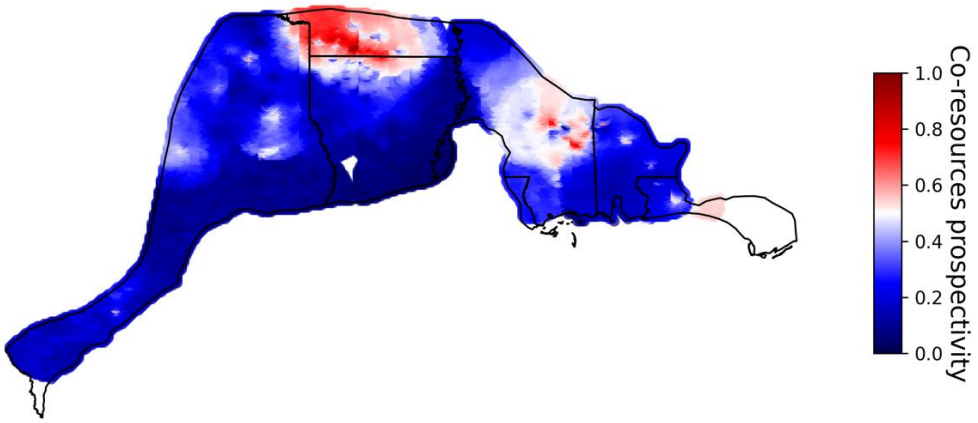


**Figure 10**: Optimistic Li and geothermal dual-resource distribution in the Smackover region based on the USGS produced water data and Stanford produced geothermal prospectivity map.

Finally, the optimistic scenario is illustrated in Figure 10, showcasing the extended potential of co-resources. It is not within our discretion to determine the preferred method; however, the two scenarios exhibit slight inconsistencies. The conservative overlap reduces the extent of co-resources, whereas the optimal overlap expands it. If the optimistic approach is adopted, we can observe a potential synergy between the two resources, which could lead to higher revenue generation.

## 4. CONCLUSIONS

The Smackover Formation holds substantial promise as a dual resource for lithium recovery and geothermal energy production, with lithium concentrations reaching up to 1,700 mg/L. However, the analysis of available datasets reveals notable variability in geochemical parameters and spatial distribution patterns. Challenges such as incomplete datasets, noisy and non-normal data distributions, and gaps in spatial coverage, particularly in southern regions, hinder comprehensive resource assessments. Addressing these limitations is essential for refining evaluations and optimizing co-extraction strategies. Advanced machine learning techniques, including nonnegative matrix factorization with k-means clustering (NMFk), have effectively identified lithium-rich zones and correlated them with geothermal characteristics. Signature 5 represents the optimal balance among tested solutions, with TDS, SG, $Cl^-$, $K^+$, and $Na^+$ showing strong correlations with lithium, indicating a robust geochemical relationship. The prospectivity distributions derived from NMFk and kriging methods exhibit strong agreement, confirming the reliability of the analysis. However, Signature 5 covers a slightly smaller extent compared to Signatures 3 and 4, reflecting spatial variations in lithium deposits. High temperatures are predominantly concentrated in the Texas region, while significant lithium resources are found in southern Arkansas and northern Louisiana, highlighting distinct geospatial

patterns. The conservative approach constrains prospectivity, while the optimistic approach expands it. If the optimistic approach is adopted, a potential synergy between the two resources becomes evident, potentially leading to higher revenue generation.

## 5. ACKNOWLEDGMENTS

This work is financially supported by the LiGRAS project from the U.S. Department of Energy Office of Energy Efficiency & Renewable Energy and Geothermal Technologies Office. This paper describes objective technical results and analysis. Any subjective views or opinions that might be expressed in the paper do not necessarily represent the views of the U.S. Department of Energy or the United States Government.

## REFERENCES

Ahmmed, B., & Vesselinov, V. V. (2022). Machine learning and shallow groundwater chemistry to identify geothermal prospects in the Great Basin, USA. Renewable Energy, *197*, 1034-1048.

Aljubran, M. J., & Horne, R. N. (2024). Thermal Earth model for the conterminous United States using an interpolative physics-informed graph neural network. Geothermal Energy, *12*(1), 25.

Attanasi, E. D., Coburn, T. C., & Freeman, P. A. (2024). Machine learning approaches to identify lithium concentration in petroleum produced waters. Mineral Economics, 1-21.

Birdwell, J. E., Whidden, K. J., Paxton, S. T., Kinney, S. A., Gardner, R. D., Pitman, J. K., ... & Schenk, C. J. (2024). Assessment of undiscovered, technically recoverable conventional oil and gas resources in the Upper Jurassic Smackover Formation, US Gulf Coast, 2022 (No. 2023-3046). US Geological Survey. Accessed December 2024

Blondes, M.S., Knierim, K.J., Croke, M.R., Freeman, P.A., Doolan, C., Herzberg, A.S., and Shelton, J.L., 2023, U.S. Geological Survey National Produced Waters Geochemical Database (ver. 3.0, December 2023): U.S. Geological Survey data release, https://doi.org/10.5066/P9DSRCZJ. https://www.sciencebase.gov/catalog/item/64fa1e71d34ed30c2054ea11 Accessed December 2024

Böttcher, A. & Wenzel, D. (2008). The frobenius norm and the commutator. *Linear algebra and its applications*, 429(8-9):1864–1885.

Cetiner, Z. S., Doğan, Ö., Özdilek, G., & Erdoğan, P. Ö. (2015). Toward utilising geothermal waters for cleaner and sustainable production: Potential of Li recovery from geothermal brines in Turkey. International Journal of Global Warming, 7(4), 439-453.

Collins, A. G. (1974). Geochemistry of liquids, gases, and rocks from the Smackover Formation (No. 7897). US Department of the Interior, Bureau of Mines.

Collins, A. G. (1969). Chemistry of some Anadarko basin brines containing high concentrations of iodide. Chemical Geology, 4(1-2), 169-187.

Darvari, R., Nicot, J. P., Scanlon, B. R., Kyle, J. R., Elliott, B. A., & Uhlman, K. (2024). Controls on lithium content of oilfield waters in Texas and neighboring states (USA). Journal of Geochemical Exploration, 257, 107363.

Dickinson, K. A. (1968). Upper Jurassic stratigraphy of some adjacent parts of Texas, Louisiana, and Arkansas. US Government Printing Office.

Ettehadi, A., Chuprin, M., Mokhtari, M., Gang, D., Wortman, P., & Heydari, E. (2024). Geological Insights into Exploration and Extraction of Lithium from Oilfield Produced-Water in the USA: A Review. Energy & Fuels.

Gibb, B. C. (2021). The rise and rise of lithium. Nature Chemistry, 13(2), 107-109.

Heydari, E., & Baria, L. (2005). A Microbial Smackover Formation and the Dual Reservoir–Seal System at the Little Cedar Creek Field in Conecuh County of Alabama.

Knierim, K. J., Blondes, M. S., Masterson, A., Freeman, P., McDevitt, B., Herzberg, A., ... & Chenault, J. (2024). Evaluation of the lithium resource in the Smackover Formation brines of southern Arkansas using machine learning. Science Advances, 10(39), eadp8149.

Kumar, A., Fukuda, H., Hatton, T. A., & Lienhard, J. H. (2019). Lithium recovery from oil and gas produced water: a need for a growing energy industry. ACS Energy Letters, 4(6), 1471-1474.

Marza, M., Ferguson, G., Thorson, J., Barton, I., Kim, J. H., Ma, L., & McIntosh, J. (2024). Geological controls on lithium production from basinal brines across North America. Journal of Geochemical Exploration, 257, 107383.

Mends, E. A., & Chu, P. (2023). Lithium extraction from unconventional aqueous resources–a review on recent technological development for seawater and geothermal brines. Journal of Environmental Chemical Engineering, 110710.

Nash, S. S. (2024). The Importance of Geology in Geothermal Development and Critical Minerals Development. In Offshore Technology Conference (p. D011S011R002). OTC.

NORAM (NORAM Engineering and Construction Ltd. (2021) Preliminary economic assessment of SW Arkansas lithium project, NI 43 – 101, Standard Lithium Ltd. Technical Report, 216 p. https://minedocs.com/21/SW-Arkansas-Lithium-Project-PEA-11202021.pdf. Accessed December 2024

Schnebele, Emily K. (2018): Bromine; Mineral Commodity Summaries 2018, U.S. Geological Survey, p. 38-39.

Sloan Jr, B. J. (1958). The Subsurface Jurassic Bodcaw Sand in Louisiana: Louisiana Geol. Sur. Bull, 33, 33.

Stringfellow, W. T., & Dobson, P. F. (2021). Technology for the recovery of lithium from geothermal brines. Energies, 14(20), 6805.

Vesselinov, V. V., Alexandrov, B. S., and O'Malley, D. (2018). Contaminant source identification using semi-supervised machine learning. Journal of contaminant hydrology, 212:134–142.

Worley (2019). Preliminary Economic Assessment of LANXESS Smackover Project, NI 43–101 Technical Report, 230pp. https://www.standardlithium.com/projects/arkansas-smackover. Accessed December 2024

Yang, S., Wang, Y., Pan, H., He, P., & Zhou, H. (2024). Lithium extraction from low-quality brines. Nature, 636(8042), 309-321.